

# Germanium Nanowire Synthesis: An Example of Solid-Phase Seeded Growth with Nickel Nanocrystals

Hsing-Yu Tuan, Doh C. Lee, Tobias Hanrath, and Brian A. Korgel\*

Department of Chemical Engineering, Texas Materials Institute, Center for Nano- and Molecular Science and Technology, The University of Texas at Austin, Austin, Texas 78712-1062

Received June 16, 2005

Germanium nanowires were synthesized by thermal decomposition of diphenyl germane in the presence of nickel (Ni) nanocrystals in supercritical toluene at 27.8 MPa and temperatures ranging from 410 to 460 °C. The growth temperature is well below the lowest Ni–Ge eutectic temperature (762 °C), and nanowire crystallization appears to occur by solid-phase alloying of the seed particle. We call this nanowire growth mechanism supercritical fluid–solid–solid (SFSS) synthesis.

## Introduction

Colloidal routes to nanomaterials synthesis can provide high-quality nanocrystals and nanowires of metals and semiconductors that can be dispersed in solvents and deposited onto substrates or incorporated into polymer composites for electronic and optical applications.<sup>1</sup> However, group IV semiconductors silicon (Si) and germanium (Ge) have been extremely challenging to synthesize in solution, with only marginal success for Si and Ge nanocrystals due to the difficulties associated with the precursor chemistry and the significant energy barrier to crystallization.<sup>2–10</sup> In 2000,<sup>11</sup> we demonstrated a high-yield crystalline Si nanowire synthesis in a high-pressure high-temperature organic solvent using diphenylsilane as a Si precursor with Au nanocrystals to seed and promote Si crystallization and later extended this approach to Ge,<sup>12</sup> GaAs,<sup>13</sup> and GaP<sup>14</sup> nanowires. Extension of the vapor–liquid–solid (VLS) mechanism from the gas phase to organic solvents requires synthetic temperatures

exceeding the Au–Si and Au–Ge eutectic temperature (both at ~360 °C), which can be achieved in solvents pressurized above their critical points—we have called this synthetic approach “supercritical fluid–liquid–solid” (SFLS) growth.<sup>15,16</sup>

Since Au forms deep electronic traps in Si and Ge, Au-seeded nanowires are relatively undesirable for electronic applications combining with Si CMOS (complementary-metal-oxide-semiconductor) technology, and other metals would be preferable as seeds. The challenge facing SFLS Ge nanowire growth using alternative metals as seeds is that the *liquid* metal–semiconductor eutectic temperatures of most of the more compatible metals with Si CMOS, such as Fe, Ni, Ti, and Co, form very high-temperature eutectics with Si and Ge<sup>17</sup>—well above the decomposition temperatures of most organic solvents (for example, 650 °C for toluene).<sup>18</sup> However, Si and Ge have very high *solid* solubility in these metals, and metal silicides commonly form by solid–solid diffusion at relatively low annealing temperatures ranging from 400 to 650 °C, depending on the material<sup>19,20</sup>—in the range accessible for supercritical organic solvents.

In a recent Letter, we reported that Ni nanocrystals promote Si nanowire synthesis in supercritical toluene at temperatures as low as 450 °C, which is more than 350 °C below the lowest temperature Ni–Si eutectic, and concluded that Ni nanocrystal-seeded Si nanowire growth can occur by a *solid-phase* seeding mechanism from the metal particle.<sup>21</sup> Here we provide further evidence supporting the occurrence of a solid-phase seeding mechanism, showing that Ni nanocrystals promote the formation of high-quality

\* Corresponding author. Phone: (512) 471-5633. Fax: (512) 471-7060. E-mail: korgel@mail.che.utexas.edu.

- (1) For a recent review, see: Law, M.; Goldberger, J.; Yang, P. *Annu. Rev. Mater. Res.* **2004**, *34*, 83–122.
- (2) Heath, J. R.; LeGoues, F. K. *Chem. Phys. Lett.* **1993**, *208*, 263–268.
- (3) Zou, J.; Baldwin, R. K.; Pettigrew, K. A.; Kauzlarich, S. M. *Nano Lett.* **2004**, *4*, 1181–1186.
- (4) Taylor, B. R.; Fox, G. A.; Hope-Weeks, L. J.; Maxwell, R. S.; Kauzlarich, S. M.; Lee, H. W. H. *Mater. Sci. Eng., B* **2002**, *96*, 90–93.
- (5) Wilcoxon, J. P.; Samara, G. A.; Provencio, P. N. *Phys. Rev. B: Condens. Matter* **1999**, *60*, 2704–2714.
- (6) Wilcoxon, J. P.; Provencio, P. P.; Samara, G. A. *Phys. Rev. B: Condens. Matter* **2001**, *64*, 035417.
- (7) Holmes, J. D.; Ziegler, K. J.; Doty, R. C.; Pell, L. E.; Johnston, K. P.; Korgel, B. A. *J. Am. Chem. Soc.* **2001**, *123*, 3743–3748.
- (8) Lu, X.; Ziegler, K. J.; Ghezelbash, A.; Johnston, K. P.; Korgel, B. A. *Nano Lett.* **2004**, *4*, 969–974.
- (9) Gerion, D.; Zaitseva, N.; Saw, C.; Casula, M. F.; Fakra, S.; Van Buuren, T.; Galli, G. *Nano Lett.* **2004**, *4*, 597–602.
- (10) Wang, W.; Huang, J.; Ren, Z. *Langmuir* **2005**, *21*, 751–754.
- (11) Holmes, J. D.; Johnston, K. P.; Doty, R. C.; Korgel, B. A. *Science* **2000**, *287*, 1471–1473.
- (12) Hanrath, T.; Korgel, B. A. *J. Am. Chem. Soc.* **2002**, *124*, 1424–1429.
- (13) Davidson, F. M., III; Schricker, A. D.; Wiacek, R. J.; Korgel, B. A. *Adv. Mater.* **2004**, *16*, 646–649.
- (14) Davidson, F. M., III; Wiacek, R.; Korgel, B. A. *Chem. Mater.* **2005**, *17*, 230–233.

- (15) Hanrath, T.; Korgel, B. A. *Adv. Mater.* **2003**, *15*, 437–440.
- (16) Shah, P. S.; Hanrath, T.; Johnston, K. P.; Korgel, B. A. *J. Phys. Chem. B* **2004**, *108*, 9574–9587.
- (17) Thaddeus, B. M.; Hiroaki, O. S. P. R.; Linda, K. *Binary Alloy Phase Diagram*, 2nd ed.; ASM International: Materials Park, OH, 1990; Vol. 1.
- (18) Lee, D. C.; Mikulec, F. V.; Korgel, B. A. *J. Am. Chem. Soc.* **2004**, *126*, 4951–4957.
- (19) Hsieh, Y. F.; Chen, L. J.; Marshall, E. D.; Lau, S. S. *Thin Solid Films* **1988**, *162*, 287–294.
- (20) Karen, M. M. V. R. *Properties of Metal Silicides*; Inspec: London, 1995.
- (21) Tuan, H.-Y.; Lee, D. C.; Hanrath, T.; Korgel, B. A. *Nano Lett.* **2005**, *5*, 681–684.

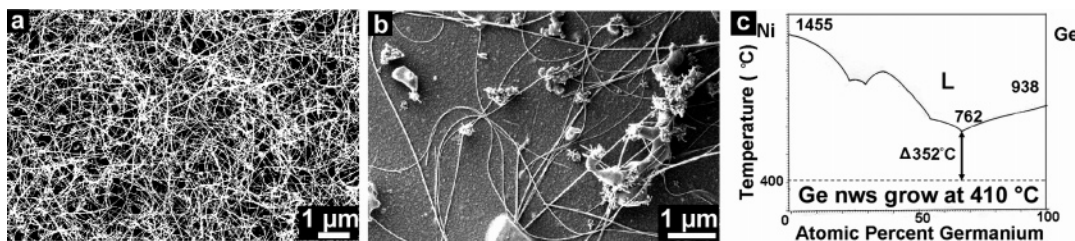


**Figure 1.** SEM images of Ni nanocrystal-seeded Ge nanowires obtained from 80 mM DPG in toluene at 27.8 MPa and (a) 460 °C and (b) 410 °C. (c) The pseudo Ni/Ge phase diagram shows the Ge nanowire synthesis temperature ("Ge nws"; dashed line) 352 °C below the lowest eutectic temperature.

crystalline Ge nanowires in organic solvents at growth temperatures approximately 350 °C below the lowest Ni–Ge eutectic temperature. These results are consistent with other recent VLS nanowire growth studies in the gas phase;<sup>22,23</sup> for example, Kamins et al., demonstrated Si nanowire synthesis from TiSi<sub>2</sub> seeds,<sup>22</sup> and Samuelson and co-workers<sup>23</sup> have proposed solid-phase seeding of GaAs nanowires from Au nanocrystals under certain conditions.

Here, we present (1) calculations of the expected diameter-dependent melting point depression showing that the Ni nanocrystals in the size range used for the Ge nanowire synthesis should be in the solid phase; (2) evidence that the quality of the nanowires depends sensitively on the NiGe<sub>x</sub> seed particle diameter with increased extended defect concentration with increasing diameter, which contrasts with the case for Au-seeded Ge nanowire synthesis; (3) measurements of the nanowire diameter distribution, revealing that it is shifted to smaller diameters relative to that of the Au-seeded synthesis due to much slower growth of larger diameter nanowires; (4) measurements of the nanowire growth rate, which relates inversely to the nanowire diameter; and (5) estimates of the solid-state diffusion rate that show that nanowire growth could proceed by either core or surface-enhanced diffusion.

### Experimental Details

**Ge Nanowire Synthesis.** Anhydrous toluene, hexane, and chloroform were purchased from Sigma-Aldrich. Diphenylgermane (DPG) was purchased from Gelest. All chemicals were used as received. Organic monolayer-coated Ni nanocrystals 5.6 ± 0.6 nm in diameter were prepared using established methods.<sup>24</sup>

Ge nanowires were synthesized in a semibatch 1 mL titanium grade-2 high-pressure reactor, heated in a brass block as described in detail by Hanrath and Korgel.<sup>12</sup> A cleaned Si wafer (4 × 30 mm<sup>2</sup>) was placed in the reactor to help collect the nanowires. The reactor was filled with toluene and sealed, then attached to a high-pressure liquid chromatography (HPLC) pump to increase the pressure and control the precursor injection rate. The reactor was flushed with anhydrous toluene for 3 min at a flow rate of 1.5 mL/min. Prior to precursor injection, the reactor was pressurized with more anhydrous oxygen-free toluene to a pressure of 3.4 MPa. Then 350 μL of toluene was injected from a 6-way valve injection loop containing 80 mM DPG and Ni nanocrystals at a Ge/Ni mole ratio of 100:1, at a flow rate 0.25 mL/min into the toluene-filled reactor at reaction temperatures ranging from 410 to 460 °C. The reactor

was pressurized further with toluene to a final reaction pressure of 27.8 MPa. The reaction was kept at temperature for 10 min. The reactor was then removed from the heating block and allowed to cool to room temperature. The reaction product appears as a dark orange-brown product, which is stored under nitrogen until use.

**Characterization Methods.** Ge nanowires were characterized using high-resolution transmission electron microscopy (HRTEM), high-resolution scanning electron microscopy (HRSEM), and energy-dispersive X-ray spectroscopy (EDS). HRSEM images were acquired on a LEO 1530 SEM equipped with a field emission gun operating between 1 and 5 kV accelerating voltage with working distances ranging between 2 and 7 mm. The nanowires were drop cast on silicon substrates for SEM imaging. HRTEM imaging was performed on a JEOL 2010F TEM at 200 kV accelerating voltage. The JEOL 2010F is equipped with an Oxford INCA ED spectrometer, which was used to acquire EDS data from nanometer-scale regions in the sample. TEM samples were prepared by drop casting nanowires from chloroform dispersion onto lacey carbon-coated TEM grids (Electron Microscopy Sciences).

### Results

**Ge Nanowire Characterization.** Figure 1a shows an SEM image of Ge nanowires obtained by decomposing DPG in the presence of Ni nanocrystals in toluene at 460 °C and 23.4 MPa. The nanowires are crystalline Ge with diamond cubic structure with few extended defects, as revealed by extensive TEM images such as those in Figure 2. The average nanowire length in a preparation is greater than 10 μm with diameters ranging from 5 to 30 nm, with most nanowires in the 5–15 nm diameter range.

Nanowires could be produced at reaction temperatures as low as 410 °C (Figure 1b), although the product yields drop off rapidly as the reaction temperature decreases. These reaction temperatures are several hundreds of degrees below the lowest Ni–Ge eutectic temperature, as seen from the phase diagram in Figure 1c.<sup>17</sup> The Ni/Ge mole ratio required for the highest quality Ge nanowires (1:100) is about an order of magnitude higher than what is needed for Au-seeded SFLS growth of Ge nanowires (1:1000) at the same DPG reaction concentration, and the optimum reaction temperature is ~80 °C higher for Ni seeding compared to that for Au seeding.<sup>12</sup> The need for these reaction conditions seems to indicate slower nanowire growth kinetics by Ni seeding compared to that of Au seeding; however, the difference in optimum synthesis temperature could simply relate to differences in Ni/Ge and Au/Ge phase compositions and temperatures, and the increased DPG decomposition rate at higher temperature may simply require a higher metal nanocrystal concentration to prevent homogeneous Ge particle formation.

The nanowire growth direction was found to be either  $\langle 110 \rangle$  or  $\langle 111 \rangle$  in approximately equal proportions, with about

(22) Kamins, T. I.; Williams, R. S.; Basile, D. P.; Hesjedal, T.; Harris, J. S. *J. Appl. Phys.* **2001**, *89*, 1008–1016.

(23) Persson, A. I.; Larsson, M. W.; Stenstroem, S.; Ohlsson, B. J.; Samuelson, L.; Wallenberg, L. R. *Nat. Mater.* **2004**, *3*, 677–681.

(24) Murray, C. B.; Sun, S.; Doyle, H.; Betley, T. *MRS Bull.* **2001**, *26*, 985–991.

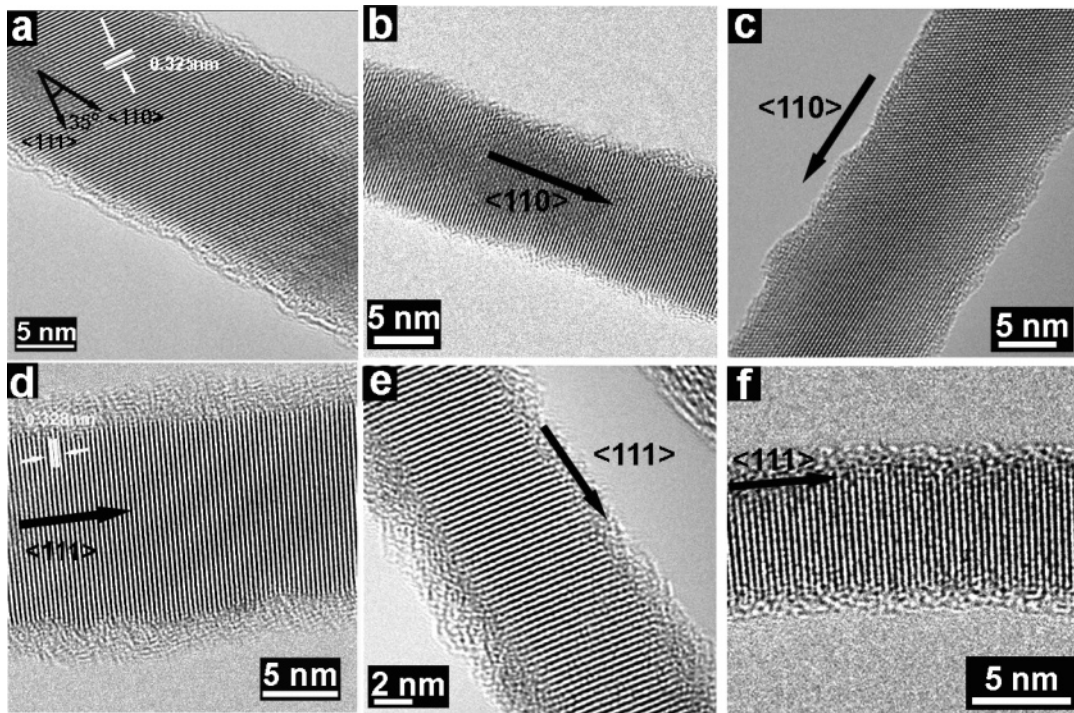


**Figure 2.** TEM images of Ni nanocrystal-seeded Ge nanowires revealing both (a–c)  $\langle 110 \rangle$  and (d–f)  $\langle 111 \rangle$  growth directions that are independent of diameter.

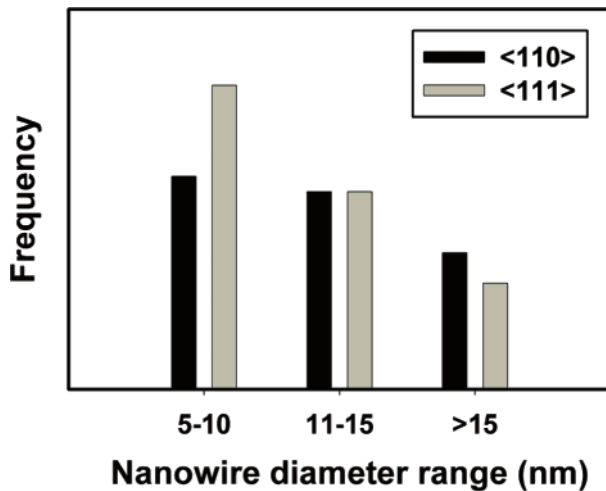


**Figure 3.** Histogram showing the relative occurrence of  $\langle 110 \rangle$  and  $\langle 111 \rangle$  oriented Ge nanowires as a function of diameter.

a 5% occurrence of  $\langle 112 \rangle$  oriented wires (3 of 83 imaged). The TEM images in Figure 2a–c show  $\langle 110 \rangle$  oriented Ge nanowires with 15.8, 10, and 13.7 nm diameters, and parts d and f in Figure 2 show Ge  $\langle 111 \rangle$  oriented nanowires with 12.6, 6.5, and 5.9 nm diameters. The observed 0.325 nm (Figure 2a) and 0.328 nm (Figure 2d) lattice spacings in the TEM images agree with the (111)  $d$ -spacing for bulk Ge (0.327 nm). Figure 3 shows a histogram of nanowire growth direction as a function of diameter obtained from HRTEM images of 80 nanowires. There is a slightly higher occurrence of  $\langle 111 \rangle$  oriented nanowires in the small size range and slightly more  $\langle 110 \rangle$  oriented wires with diameters greater than 15 nm; however, the difference in occurrence is marginal and does not appear to be statistically significant for the larger wires. These results sharply contrast SFLS-grown Ge nanowires from Au nanocrystal seeds, which

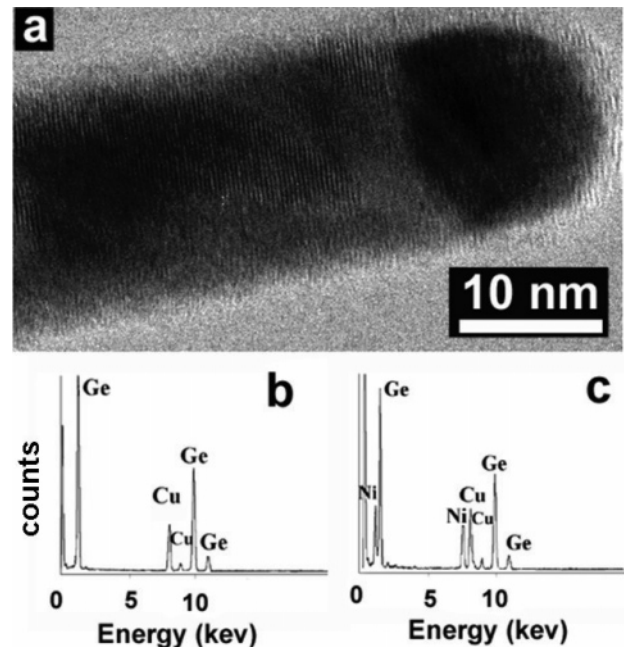


**Figure 4.** (a) TEM image of a Ni–Ge alloy seed particle at the end of a 14.5 nm Ge nanowire. Nanometer-scale EDS reveals (b) only Ge in the core of the wire and (c) Ge and Ni in the particle at the nanowire tip. The Cu signal is from background scattering off the copper grid.

exhibit  $\langle 110 \rangle$  growth directions with  $>90\%$  occurrence, regardless of diameter.<sup>25</sup>

**NiGe<sub>x</sub> Seed Particle Composition.** Ni/Ge alloy nanocrystals are found at the tip of most nanowires, as shown in the example in Figure 4. Nanobeam EDS (Figure 4, parts b and c) from the nanowire core shows only Ge, whereas EDS from the particle at the tip of the wire shows a mixture of Ni and Ge. EDS measurements of more than 30 NiGe<sub>x</sub>

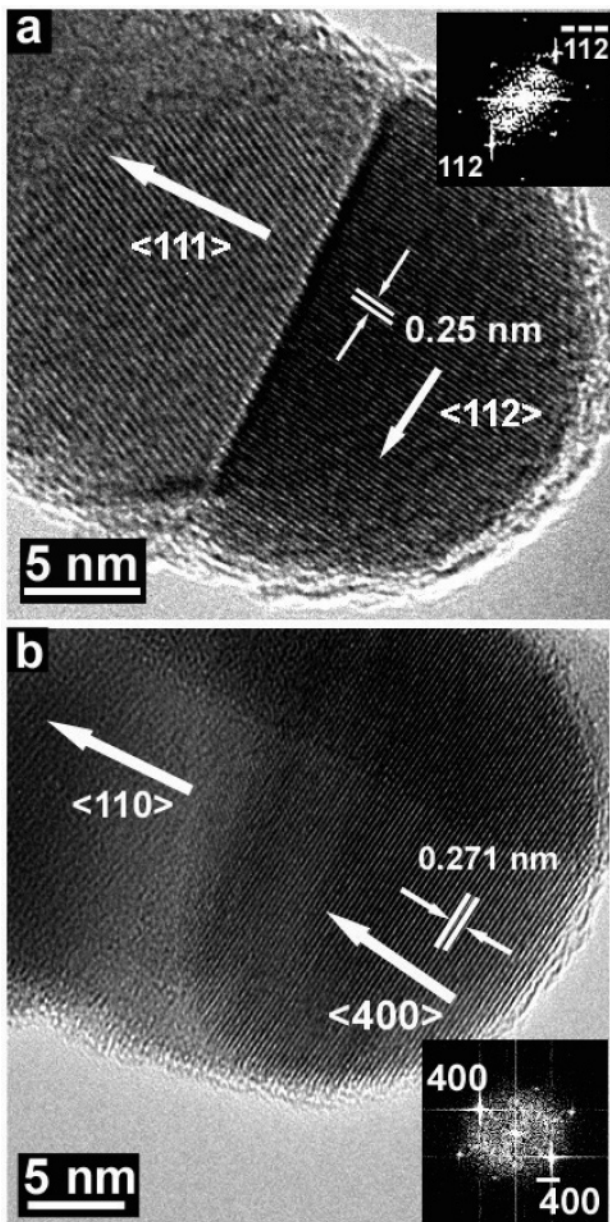


**Figure 5.** HRTEM of two NiGe<sub>2</sub> seeds at the ends of (a)  $\langle 111 \rangle$  and (b)  $\langle 110 \rangle$  oriented Ge nanowires. Insets: fast Fourier transform (FFTs) of the HRTEM images. The FFTs index to orthorhombic NiGe<sub>2</sub>, and the visible lattice spacings of (a) 0.25 nm and (b) 0.271 nm also match the NiGe<sub>2</sub> (112) and (400)  $d$ -spacings, respectively.

particles found at the tips of nanowires gave NiGe<sub>*x*</sub> alloy compositions ranging between  $1.5 < x < 2.8$ . Metal seed alloying definitely occurs during nanowire synthesis. In all cases where lattice structure could be observed in the nanocrystal at the nanowire tip (the tip needs to be oriented with the proper zone axis), as in Figure 5, parts a and b, for example, showing crystalline NiGe<sub>2</sub> particles at the tips of two Ge nanowires with different growth direction, the crystal structure (FFT pattern) and lattice spacings matched those of orthorhombic NiGe<sub>2</sub>.<sup>26</sup> It is worth noting that there was no apparent correlation between growth direction and Ni/Ge composition in the seed particle.

## Discussion

**Melting Point Depression of Ni Nanocrystals.** Nanometer diameter particles (smaller than  $\sim 20$  nm in diameter)

**Table 1.** Parameters for Ni Used to Calculate the Diameter Dependence of the Melting Temperature Using Eq 1

| parameter                                 | symbol (units)                          | solid phase           | liquid phase          |
|---|---|-----------------------|-----------------------|
| density <sup>a</sup>                      | $\rho$ (kg/m <sup>3</sup> )             | 8908                  | 8700                  |
| surface tension <sup>b</sup>              | $\gamma$ (J/m <sup>2</sup> )            | 2.28                  | 1.78                  |
|   | $\partial\gamma/\partial T^b$           | $-5.5 \times 10^{-4}$ | $-1.2 \times 10^{-3}$ |
| linear expansion coefficient <sup>b</sup> | $\alpha$ (K <sup>-1</sup> )             | $1.75 \times 10^{-5}$ | $5.26 \times 10^{-5}$ |
| latent heat <sup>a</sup>                  | $L$ (J/kg)                              | $2 \times 10^5$       |                       |
| melting temperature <sup>a</sup>          | $T_o$ (K)                               | 1728                  |                       |
| $\eta^a$                                  | $(1/\gamma)(\partial\gamma/\partial T)$ | $2.41 \times 10^{-4}$ | $6.74 \times 10^{-4}$ |

<sup>a</sup> Ref 29. <sup>b</sup> Ref 30.

exhibit a melting point depression due to the Kelvin effect. Since the nanowires are growing from seed particles in this size range, the eutectic temperature is most likely depressed making it a possibility that nanowire growth could be occurring from liquid seed droplets rather than solid seed droplets. This kind of behavior has been proposed in Au-seeded Ge nanowire growth; for example, Wang and Dai grew Ge nanowires from Au nanocrystal seeds at  $\sim 280$  °C, apparently as a result of size-dependent depression in the Au–Ge eutectic temperature,<sup>27</sup> and Hanrath and Korgel observed Au-seeded SFLS Ge nanowire synthesis at temperatures slightly below the bulk Au–Ge eutectic temperature at 300 °C.<sup>12</sup> In the case of Ni nanocrystal-seeded Ge nanowire growth, however, the Ni–Ge eutectic would need to decrease by more than 350 °C. The melting point depression for Au and Ag nanocrystals is well-known and has been measured.<sup>28</sup> The size-dependent melting point of Ni nanocrystals has not been measured but can be estimated using the modified Pawlow theory:<sup>28</sup>

$$\left(1 - \frac{T_m}{T_o}\right) - \frac{2}{L\rho_s r_c} \left[ \gamma_s - \gamma_l \left(\frac{\rho_s}{\rho_l}\right)^{2/3} \right] - \frac{2T_o}{\rho_s L r_c} \left[ \gamma_s (\eta_s - 2\alpha_s) - \gamma_l (\eta_l - 2\alpha_l) \left(\frac{\rho_s}{\rho_l}\right)^{2/3} \right] \left(1 - \frac{T_m}{T_o}\right) = 0 \quad (1)$$

In eq 1,  $r_c$  is the particle radius,  $T_o$  is the bulk melting temperature,  $T_m$  is the melting temperature of the metal particle, and the other parameters are defined in Table 1. With the use of parameters found in the literature for Ni (listed in Table 1), the melting temperature was calculated as a function of size and plotted in Figure 6. The melting temperature depression for Ni is also compared to that of Au.<sup>28</sup> Finite size effects begin to deviate from this classical approximation of the surface energy only at very small sizes—less than  $\sim 2.0$  nm diameter.<sup>28</sup>

The melting point depression for Ni nanocrystals is not as severe as that for Au. For 2 nm diameter particles, the melting point is depressed by  $\sim 80\%$  for Au but only  $\sim 20\%$  for Ni. Clearly, the Ge nanowires produced by Dai's<sup>27</sup> and Korgel's<sup>12</sup> groups at temperatures about 10% below the bulk Au–Ge eutectic temperature are possible from Au nanocrystals as large as  $\sim 12$  nm in diameter. Five nanometer diameter Ni nanocrystals are expected to have a melting point

(26) Takizawa, H.; Uheda, K.; Endo, T. *J. Alloys Compd.* **2000**, *305*, 306–310.

(27) Wang, D.; Dai, H. *Angew. Chem., Int. Ed.* **2002**, *41*, 4783–4786.

(28) Castro, T.; Reifengerger, R.; Choi, E.; Andres, R. P. *Phys. Rev. B: Condens. Matter* **1990**, *42*, 8548–8556.

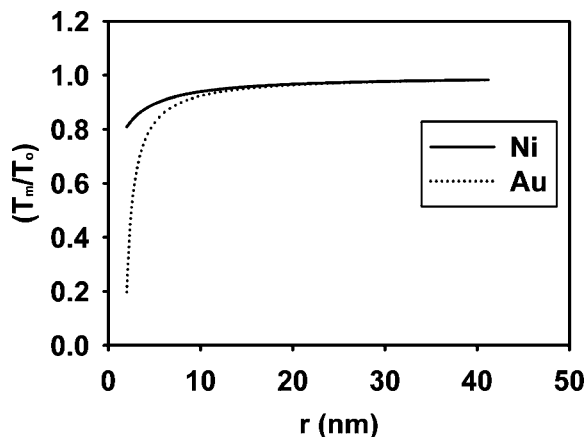


**Figure 6.** Size-dependent melting temperatures ( $T_m$ ) of Ni and Au nanocrystals (from ref 28) normalized by the bulk melting temperature ( $T_0$ ) calculated using the modified Pawlow theory (eq 1).

depression of  $\sim 10\%$ , which would drop the Ni–Ge eutectic temperature by  $\sim 100$  °C, which is still over 200 °C higher than the nanowire growth temperature. Furthermore, many of the nanowires are larger than 10 nm in diameter, which have to be growing from seeds with even less of a melting point depression. It is highly unlikely that Ni-seeded Ge nanowires grow from a liquid alloyed seed droplet at 410 to  $\sim 460$  °C.

**NiGe<sub>x</sub> Seed Particle Shape.** The shape of the NiGe<sub>x</sub> particles at the tips of the wires was observed to depend strongly on the nanowire diameter. NiGe<sub>x</sub> particles at the ends of small diameter Ge nanowires ( $< 15$  nm) were hemispherical with diameters corresponding close to the starting Ni nanocrystal size (Figure 7, parts a and b). In contrast, particles at the tips of large diameter nanowires ( $> 25$  nm) were irregularly shaped, with the appearance of a partially coalesced aggregate of nanocrystals. For example, the NiGe<sub>x</sub> particle in Figure 7d at the tip of a 32 nm diameter nanowire has an irregular cubic-faceted shape, and the NiGe<sub>x</sub> particle in Figure 7f at the end of a very large 67 nm diameter nanowire (which incidentally is very rare) has a very irregular shape. Nanobeam EDS showed that both the smaller diameter regularly shaped, and larger diameter irregularly shaped, NiGe<sub>x</sub> particles at the tips of the nanowires had a Ni/Ge ratio in the range of 1.5–2.8. Slow coalescence of large Ni particle aggregates is consistent with solid-phase seed particles. The NiGe<sub>x</sub> seed particle morphology contrasts the Au–Ge seed particles observed at the tips of Ge nanowires in the SFLS growth process. In a batch SFLS process, a very large diameter distribution can occur; for example, 2 nm diameter Au nanocrystals can produce Ge nanowires ranging from 10 to 100 nm in diameter. The Au particles at the tips of the wires, however, are all spherical regardless of the nanowire diameter, like those shown in Figure 7f. The Au–Ge particles at the tips of the wires are much more prone to aggregate and coalescence than the NiGe<sub>x</sub> particles, apparently because they are in the liquid phase.

#### Diameter Distribution of SFSS-Grown Ge Nanowires.

Figure 8 compares the Ge nanowire diameter distributions obtained using Ni and Au nanocrystals as seeds under the same reaction conditions. The Ni-seeded wires have a narrower size distribution and are much smaller than the Au-

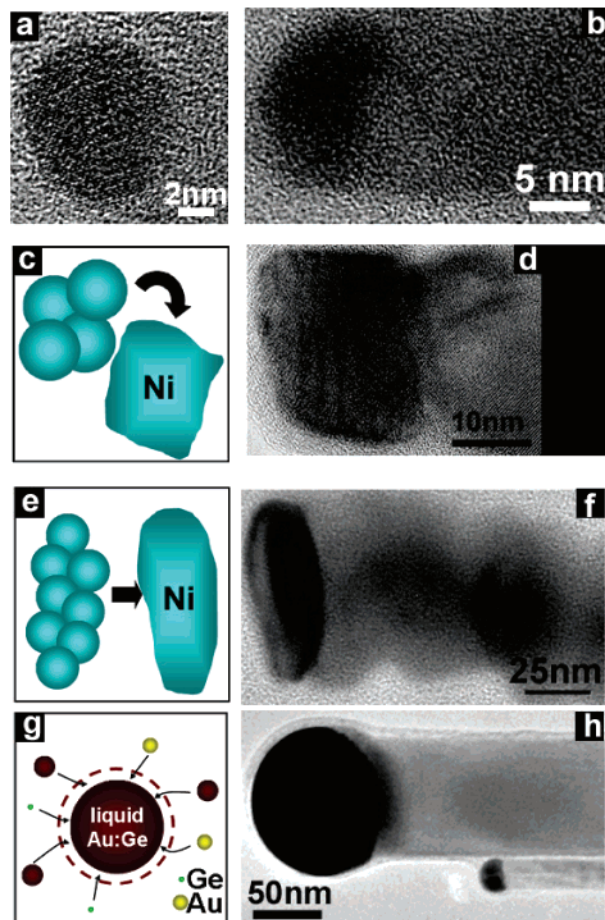


**Figure 7.** (a) TEM image of a Ni nanocrystal. (b, d, f) TEM images showing the NiGe<sub>x</sub> seed particles at the tips of Ge nanowires with increasing diameters: 15, 32, and 67 nm. (h) TEM image of Au seeds at the ends of 22 and 98 nm diameter Ge nanowires grown by SFLS. (c, e, g) Illustrations of seed particle aggregation that occurs during nanowire growth.

seeded nanowires. The Ni-seeded wires have an average diameter of 14.5 nm with more than 80% of the Ge nanowires smaller than 20 nm. The Au-seeded nanowires on the other hand are polydisperse and larger, with an average diameter of 54.8 nm. Seed particle aggregation occurs to some extent in both reactions; however, the Au nanocrystal aggregation appears to be much more significant. The Au particles form liquid Au–Ge droplets during nanowire growth that are highly susceptible to aggregation with other Au seed particles (note that this seed aggregation process must occur at the very early stages of growth since the diameters do not increase noticeably along the length of the nanowires), whereas Ni nanocrystals form a solid Ni–Ge alloy that is much less susceptible to aggregation.

There also appears to be a strong correlation between nanowire growth rate and diameter, which tends to shift the Ni-seeded Ge nanowire size distribution to smaller diameters. TEM images of the larger Ge nanowires showed large concentrations of extended defects and poor wire morphology, as in Figure 9, consistent with slow growth. Narrow diameter Ni-seeded Ge nanowires ( $< 15$  nm), however, are straight and crystalline and are much longer than the larger diameter nanowires. Larger diameter Au-seeded Ge nanowires—as large as 100 nm in diameter!—on the other hand are straight with very few extended defects (Figure 9d). Ge

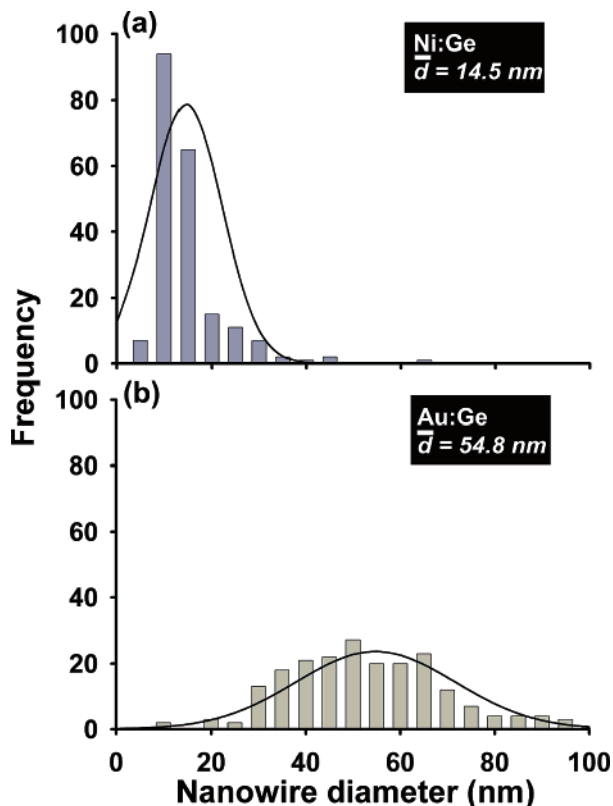


**Figure 8.** Diameter distributions of Ge nanowires synthesized in toluene at 460 °C, 23.4 MPa, and a Ge/metal mole ratio of 100:1 using (a) 5.6 nm diameter Ni nanocrystals and (b) 2 nm diameter Au nanocrystals as seeds.

diffusion through a liquid Au–Ge seed is fast, whereas solid-state diffusion limits the nanowire growth rate from NiGe<sub>2</sub> seeds when the diameter  $\sim 15$  nm.

**Diffusion-Limited Growth.** Several investigators have predicted for VLS nanowire growth that the growth rate should decrease as the diameter decreases as a result of the Kelvin effect, which lowers the supersaturation in smaller diameter nanocrystals.<sup>31,32</sup> Ni-seeded Ge nanowires, however, exhibit slower growth for larger diameter nanowires, indicating that semiconductor diffusion through the metal seed particle is limiting crystallization. From the observed nanowire growth rates, one can estimate a lower limit for the solid-phase diffusion coefficient of Ge in Ni needed for solid-phase seeding of the wires. On the basis of the observed lengths  $L$ , obtained from the reactor (consider 10  $\mu\text{m}$  with 10 min reaction time), the linear growth rate ( $dL/dt$ ) must be at least 1  $\mu\text{m}/\text{min}$  (0.017  $\mu\text{m}/\text{s}$ ). The Ge flux supplied to the tip of the solid nanowire surface,  $\text{Flux}|_{\text{surface}}$ , by diffusion through the seed metal tip to maintain this growth rate is

$$\text{Flux}|_{\text{surface}} = \rho_{\text{Ge}} \frac{dL}{dt}$$

where  $\rho_{\text{Ge}}$  is the density of Ge. The mass transfer rate at the solid nanowire surface interfaced with the metal particle can

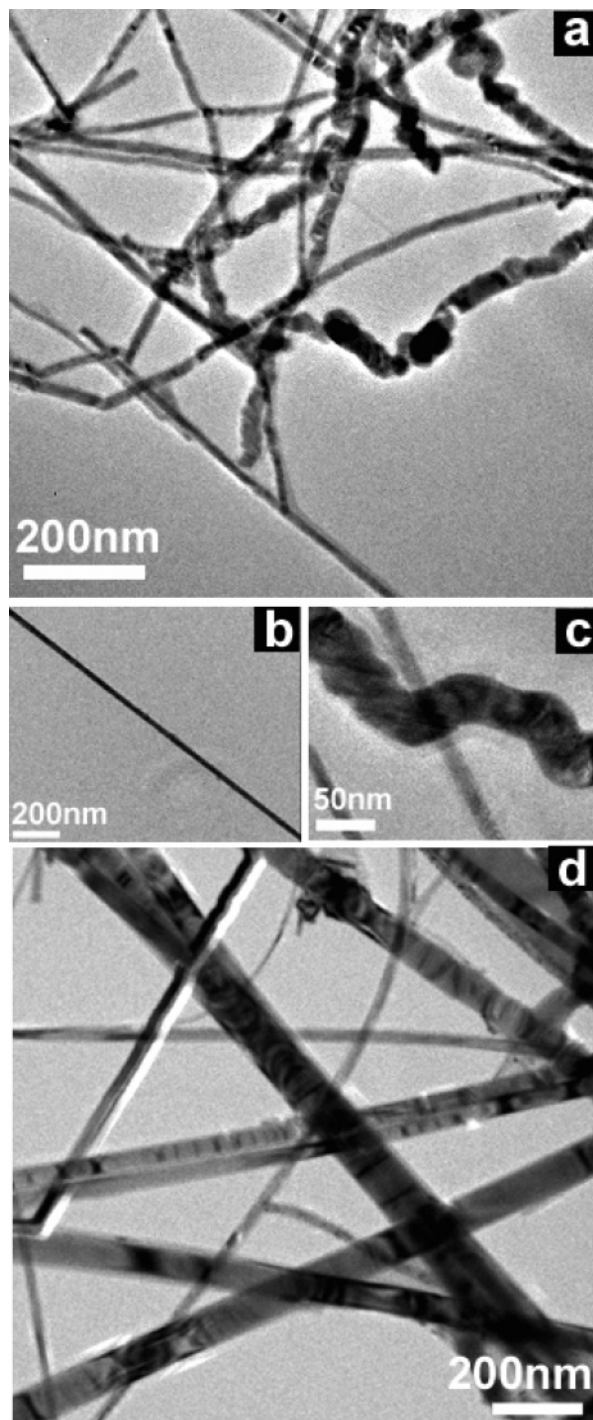


**Figure 9.** TEM images of Ge nanowires seeded by (a–c) Ni and (d) Au nanocrystals.

be estimated as<sup>33</sup>

$$\text{Flux}|_{\text{surface}} = k_m \Delta C_{\text{Ge, alloy}}$$

where  $k_m$  is the mass transfer coefficient (cm/s) and  $\Delta C_{\text{Ge, alloy}}$  is the concentration gradient of Ge in the alloyed metal tip from the solvent/metal interface to the metal/semiconductor interface. If nanowire crystallization kinetics are assumed to be much faster than the rate of Ge diffusion through the metal seed particle, then the “free” Ge concentration at the metal/semiconductor interface will be zero. If we assume

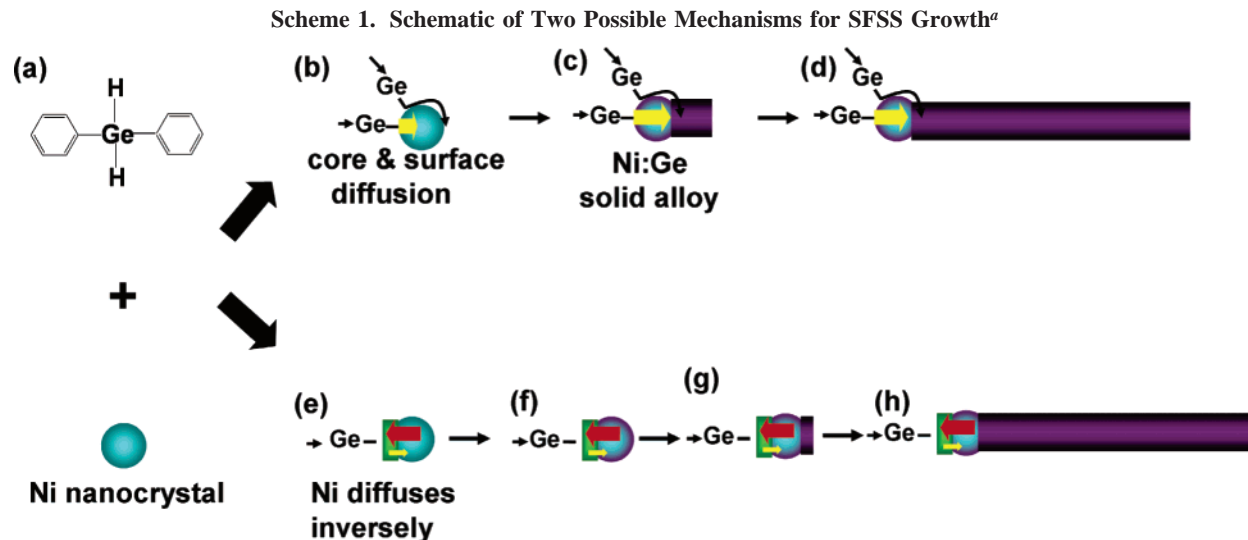
(29) *CRC Handbook of Chemistry and Physics*, 85th ed.; Lide, D. R., Ed.; CRC Press: Boca Raton, FL, 2005.

(30) Murr, E. L. *Interfacial Phenomena in Metals and Alloys*; Addison-Wesley: Reading, MA, 1975.

(31) Wu, Y.; Fan, R.; Yang, P. *Nano Lett.* **2002**, *2*, 83–86.

(32) Givargizov, E. I. *J. Cryst. Growth* **1975**, *31*, 20–30.

(33) Bird, R. B.; Stewart, W. E.; Lightfoot, E. N., *Transport Phenomena*, 2nd ed.; Wiley: New York, 2002.



the highest possible concentration gradient and take the Ge concentration at the metal/solvent interface as the concentration of pure Ge so that  $\Delta C_{\text{Ge, alloy}} \approx C_{\text{Ge, pure}} = \rho_{\text{Ge}}$ , then we see that  $k_m \geq (dL/dt)$  in order to sustain nanowire growth. For simplicity, we can estimate  $k_m$  for transport to the center of a sphere of radius  $R_{\text{sphere}}$ , which gives  $k_m = D/R_{\text{sphere}}$ , where  $D$  is the diffusion coefficient.<sup>33</sup> Although the metal seed particle is not exactly spherical and Ge is diffusing from the seed particle/solvent interface to a flat crystal surface that cross-sections the sphere, this assumption provides a good order of magnitude estimate for mass transfer of Ge from the metal/solvent interface to the metal/nanowire interface. Taking the smallest diameter nanowires observed with  $R_{\text{sphere}} = 2.5$  nm, a Ge in Ni diffusivity of  $D_{\text{Ge} \rightarrow \text{Ni}} \geq 4.25 \times 10^{-13}$  cm<sup>2</sup>/s is needed to maintain wire growth. This is about 6 orders of magnitude *faster* than the measured bulk diffusivity of Ge in Ni at 460 °C ( $D_{\text{Ge} \rightarrow \text{Ni}} = 1.79 \times 10^{-19}$  cm<sup>2</sup>/s).<sup>34</sup> However, the bulk diffusivity of Ni in Ge is *extremely fast*, with  $D_{\text{Ni} \rightarrow \text{Ge}} = 1.79 \times 10^{-7}$  cm<sup>2</sup>/s.<sup>35</sup> As DPG decomposes, Ge adsorbs to the surface of the Ni seed particles, and then Ni can counterdiffuse *into* the Ge to promote nanowire growth as illustrated in Scheme 1e–h. Another possibility is a surface-enhanced diffusion process, as shown in Scheme 1b–d, in which adsorbed Ge diffuses around the surface of the solid Ni nanocrystal to incorporate in the nanowire. This type of surface diffusion growth mechanism appears to occur for Fe nanocrystal-seeded multiwall carbon nanotube growth from supercritical toluene<sup>18,36</sup> and is a possibility; however,

Ge clearly saturates the Ni seed particle as evidenced by the NiGe<sub>2</sub> particles at the tips of the nanowires.

## Conclusions

Ni nanocrystals are effective seeds for growing Ge nanowires at temperatures well below the lowest eutectic temperature on the Ni/Ge phase diagram. Evidence indicating that the nanowires grow via a solid-phase seeding process includes model calculations, which showed that a size-dependent melting temperature depression would not be sufficient to induce melting of the NiGe<sub>x</sub> seed particles; a significant decrease in growth rate with increasing nanowire diameter; and diffusion rates of Ni into Ge that are orders of magnitude faster than those required for nanowire growth. In contrast to VLS nanowire growth, the slower growth rates for larger diameter wires focuses the diameter distribution to smaller sizes. In VLS growth, careful control of the processing parameters is needed to maintain a narrow diameter distribution,<sup>16</sup> and this represents one potential advantage of SFSS over SFLS. The wide range of alternative metals with high Si and Ge solubility makes SFSS a promising route for greatly increasing the number of metals available for seeded semiconductor nanowire growth at lower than expected processing temperatures, which is an important factor in the future integration of nanowires in devices.

**Acknowledgment.** We thank the National Science Foundation, the Welch Foundation, and the Advanced Materials Research Center in collaboration with International SEMATECH for financial support of this research. We also thank J. P. Zhou for TEM assistance.

(34) Mantl, S.; Rothman, S. J.; Nowicki, L. J.; Lerner, J. L. *J. Phys. F: Met. Phys.* **1983**, *13*, 1441–14488.

(35) Goldsmid, H. J. *Diffusion in Semiconductors*; Inspec: London, 1963.

(36) Lee, D. C.; Korgel, B. A. *Mol. Simul.*, **2005**, *31*, 637–642.